

Supporting Information

**CMOS Back-end compatible memristors for in-situ digital and
neuromorphic computing application**

Zhen-Yu He¹, Tian-Yu Wang^{1*}, Jia-Lin Meng¹, Hao Zhu^{1,2}, Li Ji^{1,2}, Qing-Qing Sun^{1,2*}, Lin Chen^{1,2*}, and David Wei Zhang^{1,2}

¹State Key Laboratory of ASIC and System, School of Microelectronics, Fudan University, Shanghai 200433, China

²National Integrated Circuit Innovation Center, No.825 Zhangheng Road, Shanghai 201203, China

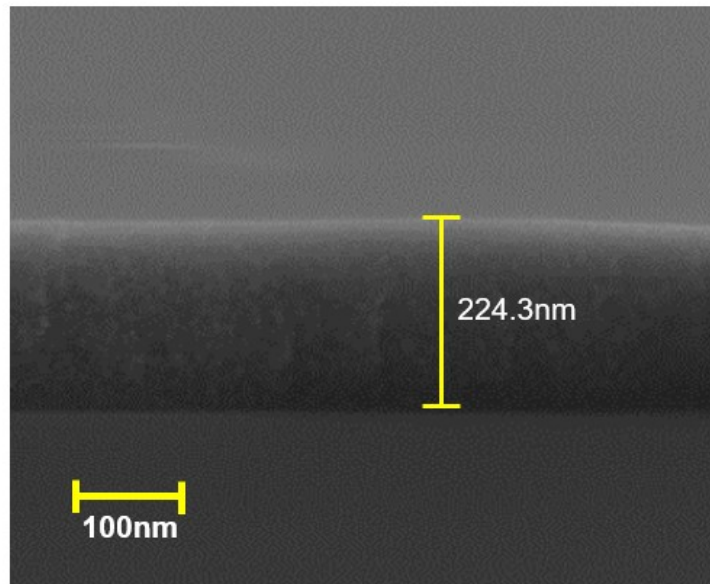


Figure S1. The SiCO:H layer grown for 8 minutes was collected by Scanning Electron Microscope (SEM), the thickness obtained by SEM and the thickness measured by SE are more consistent.

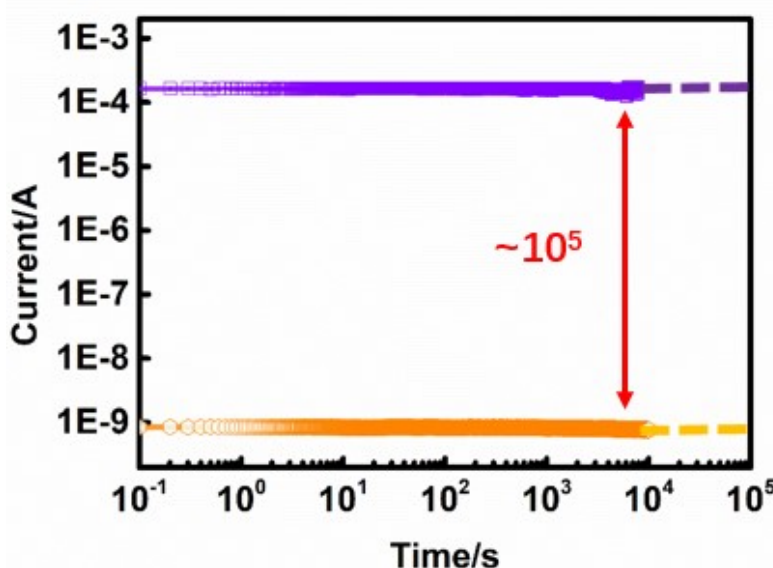


Fig.S2 The retention characteristics of Ag top electrode memristors were tested at a reading voltage of 50 mV.

Table S1 Recently reported RRAM material system based on Ag or Cu top electrode. The basic characteristics such as the threshold voltage of the device are displayed. IHRS and ILRS are the corresponding currents in high-resistance and low-resistance states, respectively.

Material system	/HRS	/LRS	ON/OFF	V _{th} (DC)	Endurance/s	Compatible with CMOS process	Ref.
Our work	30 pA	500 μA	~ 10⁵	~ 0.3V	> 10⁴	Y	
Ag/SiO ₂ /Pt	~ 1 pA	100 nA	~ 10 ⁵	~ 6 V		Y	[1]
Ag/SiO _x /C	~ 1 pA	50 uA	~ 5*10 ⁷	~ 2 V		Y	[2]
Ag/TiO ₂ /Pt		1 nA		~ 40 V		Y	[3]
Cu/SiO ₂ /Pt	~10 pA	500 μA	~ 5*10 ⁷	~ 0.6 V	> 50	Y	[4]
Cu/a-C/Pt	~ 10 uA	50 μA	5	~ 0.55V		Y	[5]
Cu/TiO _x /Pt	~ 100 pA	1 μA	~ 10 ⁴	~ 0.4 V	> 150	Y	[6]
TaN/GeO _x /HfON/Ni	~ 300 pA	100 nA	~ 9*10 ²	~ 3 V	> 10 ⁶	Y	[7]
Ag/AlO _x /Pt	~ 100 pA	100 μA	~ 104	~ 1 V		Y	[8]
Ag/a-La _{0.3} Mn _{0.7} SrO ₃ /Pt	~ 1 nA	10 μA	~ 10 ⁴	~ 0.4 V	> 100	N	[9]
Pt/Ag ₂ S/Ag/Ag ₂ S/Pt	~ 300 nA	10 μA	33	0.2 V		N	[10]
Cu/Cu-MoO _x /Pt		100 mA	~ 20	~ 2 V	> 10 ⁶	N	[11]
Pt/PCMO/Pt	~ 100 uA	1 mA	~ 100	~ 4 V	> 10 ⁴	N	[12]
Ag/Ge _x S _y /W	~ 100 pA	10 μA	~ 10 ⁵	~ 1.5 V	> 10 ⁵	N	[13]
Ag/Ta ₂ O ₅ /Fe ₃ O ₄ /Pt	~ 500 nA	5 mA	~ 10 ⁵	~ 0.4 V	> 10 ⁴	N	[14]
Ag/MXene/SiO ₂ /Pt	~ 1 uA	500 μA	~ 500	~ 0.2 V	> 10 ³	N	[15]
Ag/a-IGZO/ITO	~ 100 uA	10 mA	~ 100	~ 1.3 V	> 10 ⁶	N	[16]
Ag/ZnMn ₂ O ₄ /p-Si	~ 1 m	1 A	~ 10 ³	~ 2	> 10 ⁴	N	[17]
Pt/Ag/LZO/Pt	~ 1 uA	1 mA	~ 10 ³	~ 0.4 V	> 10 ⁴	N	[18]
Ag/Er ₂ O ₃ /ITO			~ 7	~ 2 V		N	[19]
Ag/ZrO ₂ :Cu/Pt	~ 1 nA	100 μA	~ 10 ⁵	~ 0.7 V		N	[20]

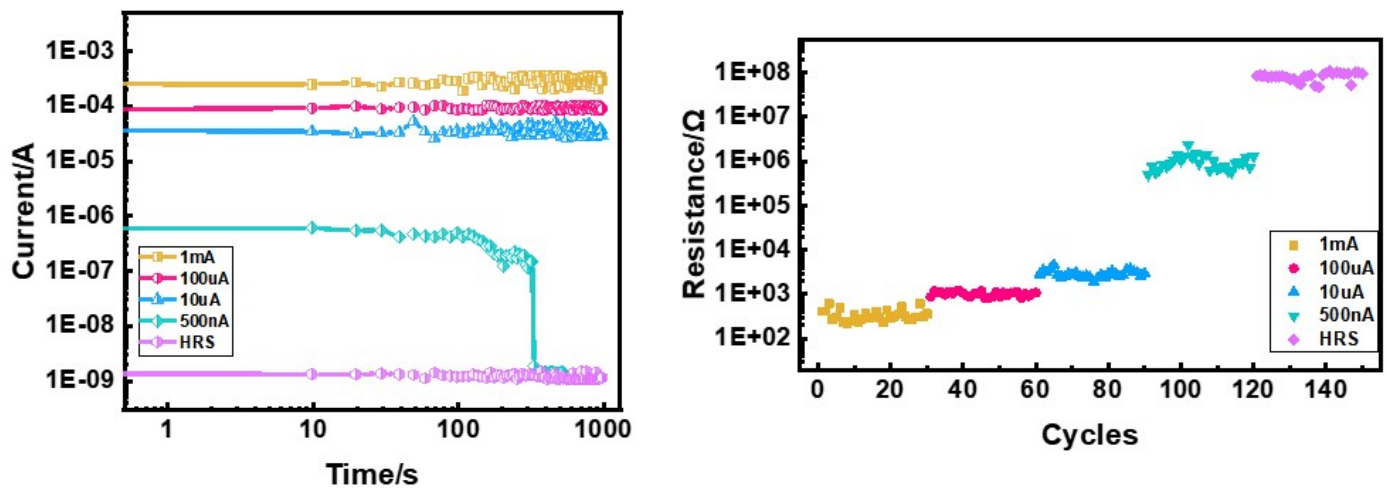


Fig.S3 (a) The retention characteristics of the Ag / SiCO:H / Pt device at different compliance levels (HRS, 500nA, 10uA, 100uA, 1mA). **(b)** The low resistance value of Ag / SiCO:H / Pt device changes under different compliance levels, showing the characteristics of the multi-resistance state. (HRS, 500nA, 10uA, 100uA, 1mA).

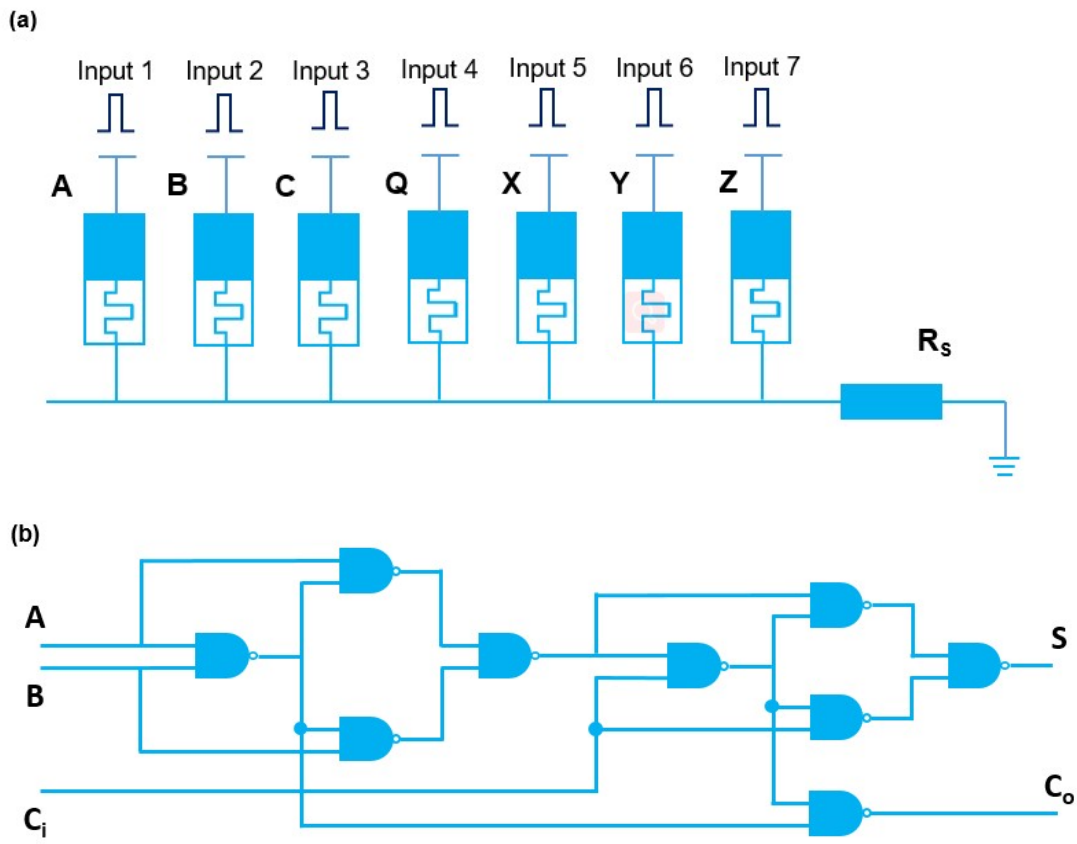


Fig.S4 (a) The circuit diagram of a one-bit full adder based on the basic logic of "IMP" based on the memristor. The circuit requires seven memristors. **(b)** The realization of a one-bit full adder logic circuit based on a traditional CMOS circuit requires 8 NAND logic to build, and each NAND logic requires 4 MOS transistors

Table S2 shows the calculation sequence of the summation S and the carry C to the higher order.

S sequence of operations	C sequence of operations
1 $X \leftarrow 1; Q \leftarrow 1$	1 $X \leftarrow 1; Y \leftarrow 1; Z \leftarrow 1$
2 $X \leftarrow A + B + C$	2 $X \leftarrow A + B$
3 $Y \leftarrow 0; Z \leftarrow 0$	3 $Y \leftarrow A + C$
4 $Y \leftarrow (B \rightarrow Y)$	4 $Z \leftarrow B + C$
5 $Z \leftarrow (C \rightarrow Z)$	5 $Y \leftarrow X \cdot Y$
6 $Q \leftarrow A + Y + Z$	6 $Y \leftarrow Z \cdot Y$
7 $Q \leftarrow X \cdot Q$	7 $C \leftarrow 1$
8 $X \leftarrow 0$	8 $C \leftarrow Y \cdot C$
9 $X \leftarrow (A \rightarrow X)$	
10 $Z \leftarrow X + Y + C$	
11 $Q \leftarrow Z \cdot Q$	
12 $Y \leftarrow 0$	
13 $Z \leftarrow B + X + Y$	
14 $Y \leftarrow (C \rightarrow Y)$	

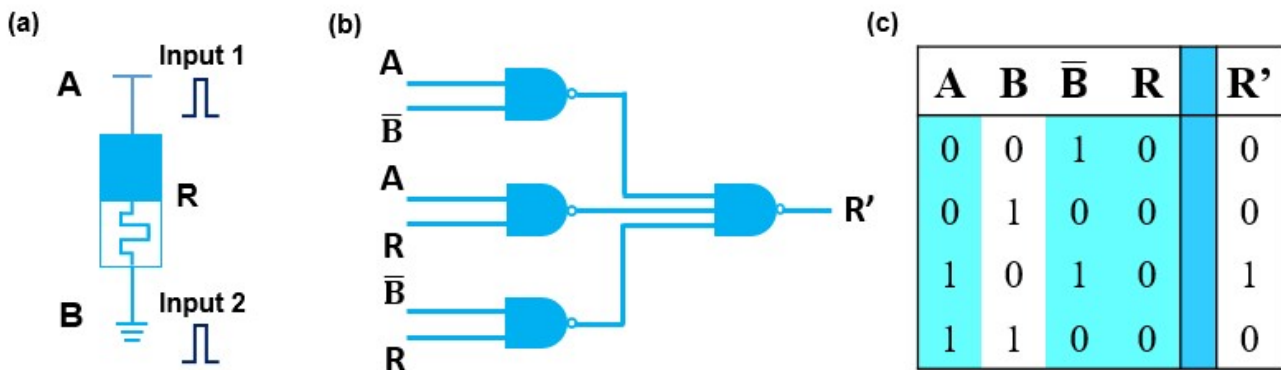


Fig.S5. (a) One memristor can realize "MIG" logic. (b) A circuit that implements a multi-bit voter based on a traditional CMOS circuit requires a total of four NAND logic, and each NAND logic requires four MOS transistors. (c) Supplement to the truth table of MIG logic in the original text.

Reference

- [1] Sun, H.; Liu, Q.; Li, C.; Long, S.; Lv, H.; & Bi, C.; et al. Memory switching: direct observation of conversion between threshold switching and memory switching induced by conductive filament morphology. *Advanced Functional Materials* **2014**, 36.
- [2] Bricalli, A.; Ambrosi, E.; Laudato, M.; Maestro, M.; & Bricalli, A.; SiOx-based resistive switching memory (RRAM) for crossbar storage/select elements with high on/off ratio. *2016 IEEE International Electron Devices Meeting (IEDM)* **2017**.
- [3] Hsiung, C. P.; Liao, H. W.; Gan, J. Y.; Wu, T. B.; Hwang, J. C.; & Chen, F.; et al. Formation and instability of silver nanofilament in ag-based programmable metallization cells. *Acs Nano*, **2010**, 4(9), 5414-5420.
- [4] Chen, W.; Barnaby, H. J.; & Kozicki, M. N.; Volatile and non-volatile switching in cu-sio2 programmable metallization cells. *IEEE Electron Device Letters* **2016**, 37(5), 580-583.
- [5] X. Zhao.; H. Xu.; Z. Wang.; L. Zhang.; J. Ma.; & Y. Liu.; Nonvolatile/volatile behaviors and quantized conductance observed in resistive switching memory based on amorphous carbon. *Carbon* **2015**.
- [6] J. Woo.; D. Lee.; E. Cha.; S. Lee.; S. Park.; H. Hwang.; Effects of reset current overshoot and resistance state on reliability of rram. *IEEE Electron Device Letters* **2014**, 35, 60.
- [7] Cheng, C. H.; Chin, A.; Yeh, F. S.; Ultralow Switching Energy Ni/ /HfON/TaN RRAM. *Electron Device Letters, IEEE* **2011**, 32(3):p.366-368.
- [8] Yuan, F.; Zhang, Z.; Wang, J. C.; et al. Total ionizing dose (TID) effects of γ ray radiation on switching behaviors of Ag/AlO x /Pt RRAM device. *Nanoscale Research Letters* **2014**, 9(1):1-6.

- [9] D, Liu.; Cheng, H.; Wang, G.; Xuan, Z.; & Wang, N.; Diode-like volatile resistive switching properties in amorphous sr-doped lamno₃ thin films under lower current compliance. *Journal of Applied Physics* **2013**, 114(15), 154906-154906-5.
- [10] Woo, J.; Hwang, H.; Communication-Comprehensive Assessment of a Back-to-Back Schottky Diode with Ultrathin TiO₂ Layer for Cross-Point Selector Applications. *Ecs Journal of Solid State Science & Technology* **2016**, 5(6):Q188-Q190.
- [11] D, Lee.; Excellent uniformity and reproducible resistance switching characteristics of doped binary metal oxides for non-volatile resistance memory applications. *IEEE 2007*.
- [12] Jo, M.; Seong, D.J.; Kim, S.; Novel cross-point resistive switching memory with self-formed schottky barrier *Symposium on Vlsi Technology IEEE 2010*, 53-54.
- [13] Wei, L.; Doo, S J.; Michael K.; and Rainer W.; Electrochemical metallization cells—blending nanoionics into nanoelectronics? *Mrs Bulletin* **2012**.
- [14] Chang, C. F.; Chen, J. Y.; Huang, G. M.; Lin, T. Y.; Tai, K. L.; Huang, C. Y.; Yeh, P. H.; Wu, W. W.; Revealing Conducting Filament Evolution in Low Power and High Reliability Fe₃O₄/Ta₂O₅ Bilayer RRAM. *Nano Energy* **2018**, 53:S2211285518306736-.
- [15] Lian, X.; Shen, X.; Fu, J.; et al. Electrical Properties and Biological Synaptic Simulation of Ag/MXene/SiO₂/Pt RRAM Devices. *Electronics*, **2020**, 9(12):2098.
- [16] Chen, Z. H.; Liu, Z.; Ma, W. K.; et al. Resistive switching characteristics of RRAM devices based on spin-coated a-IGZO thin films and ink-jet printed Ag electrodes. *Nanoelectronics Conference IEEE 2016*.
- [17] Wang, H.; Li Z.; Xu J.; et al. Resistance switching properties of Ag/ZnMn₂O₄/p-Si fabricated by magnetron sputtering for resistance random access memory[J]. *Journal of Wuhan University of Technology-Mater. Sci. Ed.* 2015.
- [18] Zhao, X.; Song, P.; Gai, H.; et al. Li-Doping Effect on Characteristics of ZnO Thin Films Resistive Random Access Memory. *Micromachines* **2020**, 11(10).
- [19] Mao, S.; Zhou, G.; Sun, B.; et al. Mechanism analysis of switching direction transformation in an Er₂O₃ based RRAM device. *Current Applied Physics* **2019**, 19(12).
- [20] Long, S.; Qi, L.; Lv, H.; et al. Resistive switching mechanism of Ag/ZrO₂:Cu/Pt memory cell. *Applied Physics A* **2011**, 102(4):915-919.